

Acoustic Coherent Backscatter Enhancement from Aggregations of Point Scatterers

David R. Dowling
Department of Mechanical Engineering
University of Michigan
Ann Arbor, MI 48109-2133
phone: (734) 936-0423 fax: (734) 764-4256 email: drd@umich.edu

Award #: N00014-11-1-0258
<http://www.personal.engin.umich.edu/~drd/>

LONG-TERM GOALS

The overall long-term goal for this project is to determine if and how acoustic coherent backscatter enhancement (ACBE) can be used for classification of active sonar returns in a wide variety of ocean environments. During its first four years, this project has focused on simulations of near- and far-field acoustic multiple scattering from two- and now three-dimensional aggregations of omnidirectional point scatterers to determine the parametric realms in which ACBE might be observed, and its characteristics when it is observed.

OBJECTIVES

The detailed objectives of the current research effort are to determine the parametric dependence of ACBE peak amplitude, peak emergence rate as the number of observations increases, peak angular width, and peak time dependence. Here the independent parameters are the range between the scattering aggregation and the receiving array, the receiving array characteristics, incident wave characteristics (wave front shape, waveform, frequency, bandwidth, duration), and aggregation characteristics (scatterer cross section and mean spacing, overall aggregation size and shape, etc.). Eventually, underwater waveguide characteristics will be considered as well.

APPROACH

The current approach involves numerical evaluation of the fundamental equations of multiple scattering from an aggregation of omnidirectional point scatterers [1]. If $\psi(\mathbf{r})$ is the harmonic acoustic pressure field at frequency ω at the point \mathbf{r} and $\psi_0(\mathbf{r})$ is the harmonic field incident on the aggregation of scatterers located at \mathbf{r}_n , then

$$\psi(\mathbf{r}) = \psi_0(\mathbf{r}) + \psi_s(\mathbf{r}) = \psi_0(\mathbf{r}) + \sum_{n=1}^N g_n \psi_n(\mathbf{r}_n) G(\mathbf{r}, \mathbf{r}_n), \quad (1)$$

where $\psi_s(\mathbf{r})$ is the scattered field and is given by the sum in (1), N is the number of scatterers, g_n is the scattering coefficient of the n^{th} scatterer, $\psi_n(\mathbf{r}_n)$ is the field incident on the n^{th} scatterer,

$$\psi_n(\mathbf{r}_n) = \psi_0(\mathbf{r}_n) + \sum_{j=1, j \neq n}^N g_j \psi_j(\mathbf{r}_j) G(\mathbf{r}_n, \mathbf{r}_j) \quad (2)$$

and $G(\mathbf{r}_n, \mathbf{r}_j)$ is the free-space Green's function between the locations \mathbf{r}_n and \mathbf{r}_j ,

$$G(\mathbf{r}_n, \mathbf{r}_j) = \frac{\exp\{-ik|\mathbf{r}_n - \mathbf{r}_j|\}}{|\mathbf{r}_n - \mathbf{r}_j|} \quad (3)$$

where $k = \omega/c$ is the wave number magnitude of the incident field, c is the sound speed, and $i = \sqrt{-1}$. When the incident field and the scattering coefficients are known, (2) can be written N times, once for each scatterer $1 \leq n \leq N$, and these N algebraic equations can be solved to determine $\psi_n(\mathbf{r}_n)$. The total field at any location is then recovered from (1) and (3) using the known $\psi_0(\mathbf{r})$, the known g_n , and the calculated $\psi_n(\mathbf{r}_n)$.

In the current investigation, the scatterers are placed randomly with an average spacing s , and are identical. For the calculations without internal losses in the scatterers, the N scattering coefficients are the same:

$$\mathbf{g}_n = \mathbf{g}_1 = \left(\frac{\sigma_s}{4\pi} - \frac{k^2 \sigma_s^2}{16\pi^2} \right)^{1/2} - i \frac{k\sigma_s}{4\pi}, \quad (4)$$

where σ_s is the scattering cross section. In the current investigations, σ_s is considered an independent parameter within the constraint imposed by conservation of acoustic energy: $\sigma_s \leq 4\pi/k^2 = \lambda^2/\pi$. For the current calculations, the incident field $\psi_0(\mathbf{r})$ is a plane wave with amplitude A and wave number vector \vec{k} , and the backscatter direction ($\phi = \varphi = 0$) is defined with respect to \vec{k} as shown in Figure 1. For calculations including internal losses within the scatterers, (4) is replaced with

$$\mathbf{g}_n = \mathbf{g}_1 = \left(\frac{\sigma_s}{4\pi} - \frac{k^2(\sigma_c + \sigma_s)^2}{16\pi^2} \right)^{1/2} - i \frac{k(\sigma_c + \sigma_s)}{4\pi}, \quad (5)$$

where σ_c is the absorption (or capture) cross section of each scatterer (see [1]).

To search for the presence or absence of ACBE, the scattered field $\psi_s(\mathbf{r})$ predicted by (1) is calculated at the elements of the receiving array, and aggregation-array distance R is varied to put the receiving array in the near-field, where the array's beam-steering angle ϕ is relevant, or in the far-field of the aggregation, where the azimuthal (or bistatic) scattering angle φ is relevant. For near-field calculations, the results are presented as $B(\phi)/[B]_{not\ peak}$ vs. ϕ , where $B(\phi)$ is the beamformed output of the receiving array, and $[B]_{not\ peak}$ is the array's average beamformed output in directions near backscatter but excluding the ACBE peak. The independent parameters of these investigations are A , k , σ_s , σ_c , s , R , L , ϕ or φ , and parameters associated with aggregation's size and shape.

The focus of this research effort during FY 15 was on determining and understanding the parametric dependence of the ACBE peak's characteristics in the near field and far field of aggregations with readily defined shapes. In particular, the current simulations show the near-field ACBE peak width is set by the dimensionless length kL of the receiving array, while the near-field ACBE peak enhancement depends on a combination of $k\sigma_s^{1/2}$ and ks .

These ACBE investigations are the current doctoral research of Ms. Adaleena Mookerjee. She is a US Citizen and a Ph.D. candidate.

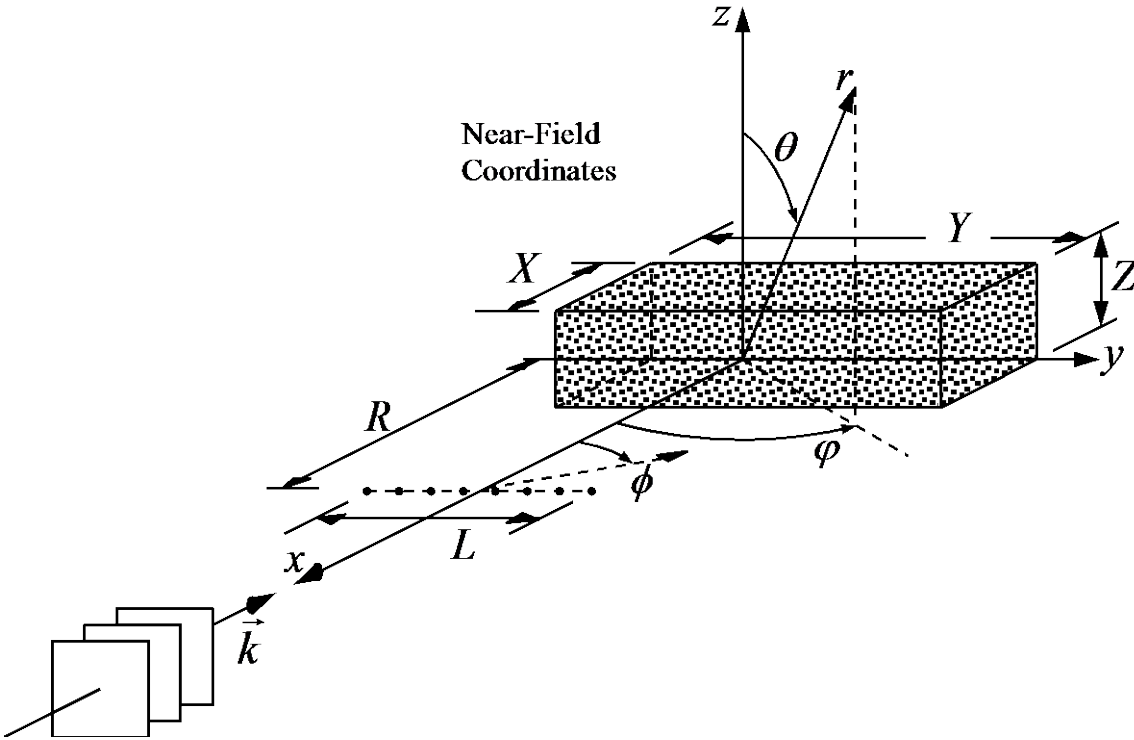


Figure 1. Geometrical configuration of the multiple scattering simulations. A plane wave with amplitude A and wave number vector \vec{k} impinges on a rectangular aggregation of scatterers with dimensions X , Y , and Z . Here θ is the scattering angle defined from the origin of coordinates, and ϕ is the beam-steering angle defined from the broadside direction of the receiving array of length L that lies a distance R from the aggregation. The backscatter direction is $\theta = \phi = 0$.

WORK COMPLETED

During FY15 the final code validation tasks were completed [2]. Then, ACBE was simulated for three-dimensional rectangular, spherical, oblate spheroidal, and prolate spheroidal aggregation shapes. Both near-field and far-field scattering geometries were studied. In addition, broadband ACBE simulations of acoustic scattering from aggregations of ideal scatterers have been completed, and similar simulations from schools of herring, yellow fin tuna, and lantern fish in ideal aggregation shapes with realistic scatterer properties and aggregation sizes are now underway.

RESULTS

The final validation test for the simulations involved near-field ACBE simulations that mimicked the experiments of Bayer and Niederdränk [3] who measured ultrasound backscatter from gravel stones submerged in water and having a wave number scaled average diameter of $kd = 50.3$. In this parametric range the scattering is nearly omnidirectional away from the forward direction. The mean free path provided by Bayer and Niederdränk (1993) was $kl = 69.2$, and the aggregation geometry was semi-infinite with depth and width larger than the mean free path.

To simulate this experiment, the aggregation geometry shown in Fig. 1 was used with $N = 5400$, and dimensions of $kX = 20$, $kY = 100$, and $kZ = 20$. Here, to expedite the simulation convergence (only 256-330 realizations were needed), the average scatterer spacing was reduced to $ks = 1.95$ and the scatterer strength was set to $k\sigma_s^{1/2} = 0.70$ to achieve a mean free path of $kl = 69.6$ (very close to the experimental value). In addition, a linear taper was added to the shadowed side of the aggregation from $-40 \leq kx \leq -20$, adding 2000 more scatterers to the back of the aggregation. Here, fully near-field results were obtained from repeated simulations with kR decreasing. Figure 2 shows the change in $B(\phi)/[B(\phi)]_{not\ peak}$ vs. the beam steering angle ϕ for decreasing values of $kR = 18.2$ (- - - -), 15.2 (- • - • -), 13.2 (- - - -), 11.2 (- - - -), 8.2 (- • - • -) and 5 (••••••••). For comparison, the Bayer and Niederdränk (1993) experimental results (Fig. 5 in their paper) are centered (a shift of 1.5°) and plotted as the solid curve. The simulation results for $kR = 8.2$ and 5 are both well matched to the shifted experimental results with all three providing an ACBE peak of 1.5. These results show that the current simulations agree with acoustic CBE experimental results when the mean free path in the scattering aggregation is matched and the angular resolutions of the experiments and simulations are comparable.

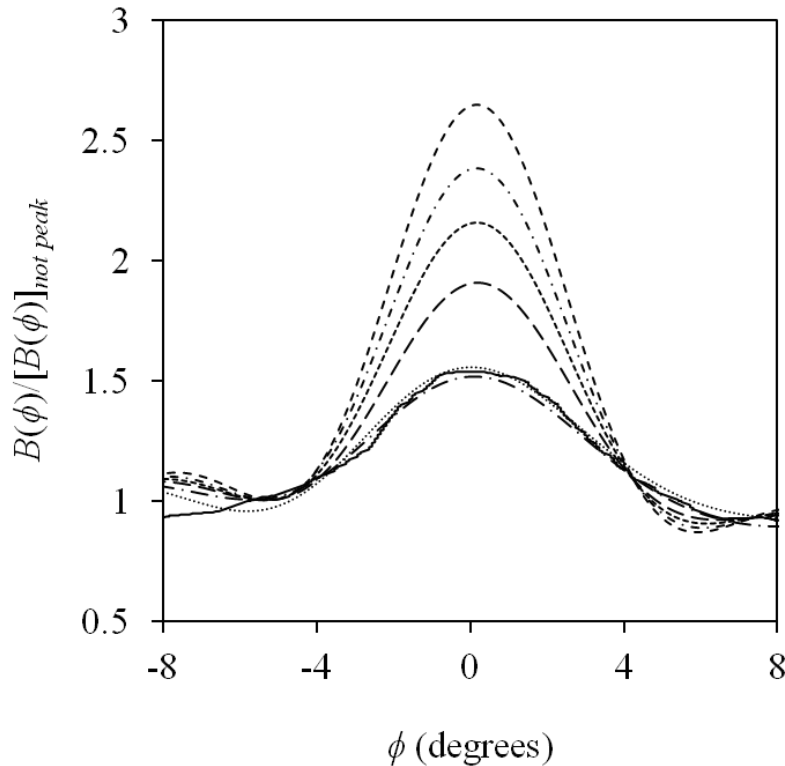


Figure 2. Ensemble-averaged beamformed intensity ratio, $B(\phi)/[B(\phi)]_{not\ peak}$ vs. the beam steering angle ϕ for decreasing values of $kR = 18.2$ (- - - -), 15.2 (- • - • -), 13.2 (- - - -), 11.2 (- - - -), 8.2 (- • - • -) and 5 (••••••••) using the scattering geometry shown in Figure 1. The experimental results from [3] are shown as a solid curve and match the simulation results from $kR = 5$, and 8.2.

When the validation of the simulation code was complete, it was used to perform a parameter study using a fixed scattering geometry and aggregation size but variable wave-number-scaled scatterer spacing ks and scattering strength, here represented by $k\sigma_s^{1/2}$. A total of 24 different simulations were completed with $kR = 18.2$, $kL = 64$, $kX = 64$, $kY = 100$, and $kZ = 20$ that spanned the parametric ranges: $2.9 \leq ks \leq 6.4$ and $0.032 < k\sigma_s^{1/2} < 3.544$. Then, CBE peak height ($= B(0)/[B(\phi)]_{not\ peak}$) was plotted vs.

simple algebraic combinations of ks and $k\sigma_s^{1/2}$ to look for a combination that would collapse the ACBE peak height results to a single curve. The result of this effort is shown in Fig. 3, and is interesting for at least two reasons. First, it suggests that any parametric change that increases $(k^2\sigma_s)^{1/4}(ks)^{-1}$ will also increase the prominence of the acoustic CBE peak. And second, these results clearly show that CBE peak height may exceed two when the aggregation is of finite size. These facts may have important implications for remote sensing of aggregations of scatterers.

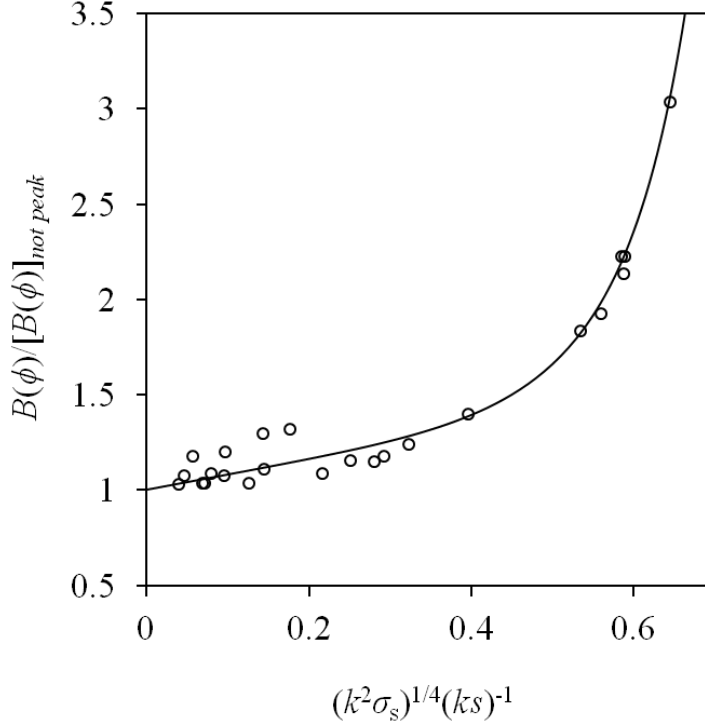


Figure 3. Simulated acoustic CBE peak heights $B(\phi)/[B(\phi)]_{not\ peak}$ versus $(k^2\sigma_s)^{1/4}(ks)^{-1}$ when $kX = 64$, $kY = 100$, and $kZ = 20$, $2.9 \leq ks \leq 6.4$ and $0.032 \leq k\sigma_s^{1/2} \leq 3.544$ for $kR = 18.2$. The simulated peak height increases approximately monotonically with $(k^2\sigma_s)^{1/4}(ks)^{-1}$. The mild scatter of the points is caused by the residual effects of the finite-sized scattering aggregation and the fact that the peak height ratio may depend separately on ks and $k^2\sigma_s$ while the product $(k^2\sigma_s)^{1/4}(ks)^{-1}$ combines these parameters.

Sample broadband mean-square-pressure simulation results are shown on Figure 4 for 64 realizations of far-field scattering from a 2.5-m-radius spherical aggregation of 1000 elastic scatterers illuminated by a 100-ms-duration 3 kHz to 4 kHz frequency-sweep pulse. At the center frequency of the pulse, the wave number scaled sizes are: $k(\text{sphere's radius}) = 36.7$, $k\sigma_s^{1/2} = 2.5$, and $ks = 5.9$. In Fig. 4, the color scale is linear (not dB), the bistatic scattering angle (ϕ , see Fig. 1) is on the vertical axis, the horizontal axis is time with $t = 0$ corresponding to the time when the pulse hits the aggregation. Here the presence of ACBE is indicated by the concentration of red fringes within $\pm 10^\circ$ or so of the backscatter direction ($\phi = 0$). Simulations like these may provide time-domain classification clues for determining the difference between an aggregation of many small scatterers and a single large scatterer.

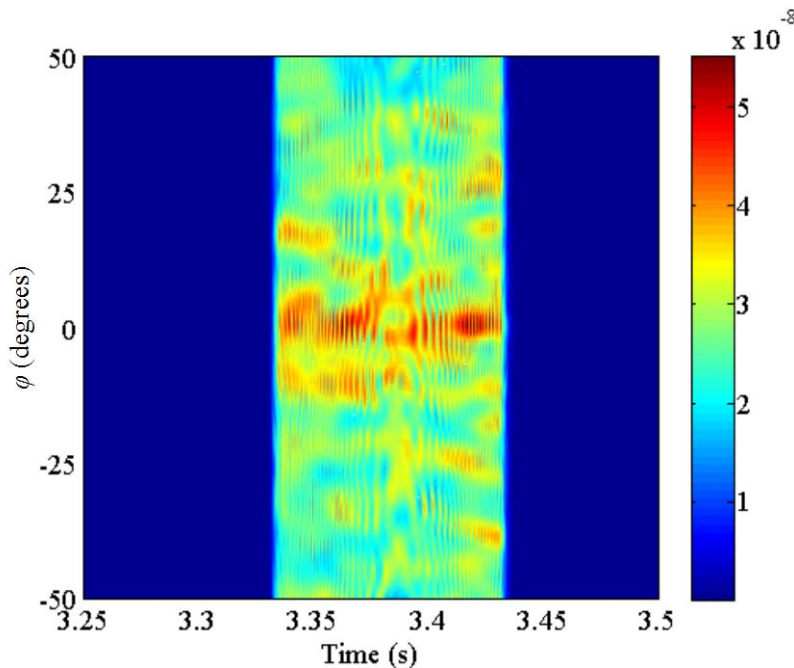


Figure 3. Ensemble average of 64 broadband simulations of the far-field mean-square acoustic pressure scattered from a spherical aggregation of 1000 randomly-placed elastic scatterers. The incident waveform is a 100-ms-duration 3 kHz to 4 kHz frequency-sweep pulse. Here φ is the bistatic scattering angle defined in Fig. 1 and the scattered field exists in the time interval $3.33s < t < 3.43s$. The red fringes within $\pm 10^\circ$ or so of $\varphi = 0$ indicate the presence of ACBE.

IMPACT/APPLICATION

In broad terms, this project ultimately seeks to determine if and how ACBE might be exploited for active sonar applications. In particular, if successful, it should prove useful for remote classification, because a large sonar return from a single large scatterer will likely not display ACBE while a similarly large sonar return from an aggregation of many small scatterers may display ACBE. Thus, this research effort may eventually impact how active sonar signals are processed and displayed for tactical decision-making related to classification.

TRANSITIONS

The results of this research effort should aid in the design of active sonar signal processors for tactical decision aids. However, at this time no direct transition links have been established with more applied research programs. Once the current simulation capability has been more fully exploited for parameter studies, and promising results have been obtained, a transition path through NRL or one of the Navy's Warfare Centers will be sought.

RELATED PROJECTS

This project is related to the other projects funded under ONR's 2010 basic research challenge program. In particular, the efforts by Prof. Feuillade in Chile and Prof. Sabra at Georgia Tech are most closely related.

REFERENCES AND PUBLICATIONS

- [1] Foldy, L.L. (1945) "The multiple scattering of waves, I. General theory of isotropic scattering by randomly distributed scatterers," *Physical Review* Vol. 67, 107-119.
- [2] Mookerjee, A. and Dowling, D.R. (2015) "Simulating acoustic coherent backscattering enhancement from random aggregations of omnidirectional scatterers" *J. Acoustic. Soc. Am.* Vol. 138, 758-768.
- [3] Bayer, G., & Niederdränk, T. (1993) "Weak localization of acoustic waves in strongly scattering media" *Phys. Rev. Letters* Vol. 70, 3884-3887.